



HAL
open science

OTFS-IM channel estimation and data detection algorithm with a superimposed pilot pattern

Rabah Ouchikh, Abdeldjalil Aissa El Bey, Thierry Chonavel, Mustapha Djeddou

► **To cite this version:**

Rabah Ouchikh, Abdeldjalil Aissa El Bey, Thierry Chonavel, Mustapha Djeddou. OTFS-IM channel estimation and data detection algorithm with a superimposed pilot pattern. SSP 2023: IEEE Statistical Signal Processing workshop, Jul 2023, Hanoi, Vietnam. 10.1109/SSP53291.2023.10207981 . hal-04080284

HAL Id: hal-04080284

<https://imt-atlantique.hal.science/hal-04080284>

Submitted on 24 Apr 2023

HAL is a multi-disciplinary open access archive for the deposit and dissemination of scientific research documents, whether they are published or not. The documents may come from teaching and research institutions in France or abroad, or from public or private research centers.

L'archive ouverte pluridisciplinaire **HAL**, est destinée au dépôt et à la diffusion de documents scientifiques de niveau recherche, publiés ou non, émanant des établissements d'enseignement et de recherche français ou étrangers, des laboratoires publics ou privés.



Distributed under a Creative Commons Attribution 4.0 International License

OTFS-IM channel estimation and data detection algorithm with a superimposed pilot pattern

Rabah Ouchikh Abdeldjalil Aïssa-El-Bey Thierry Chonavel Mustapha Djeddou
Lab Télécommunications *IMT Atlantique, Lab-STICC,* *IMT Atlantique, Lab-STICC,* *Lab Télécommunications*
Ecole Militaire Polytechnique *UMR CNRS 6285, F-29238,* *UMR CNRS 6285, F-29238,* *Ecole Militaire Polytechnique*
Bordj El-Bahri, Algeria Brest, France Brest, France Bordj El-Bahri, Algeria
ouchikh16rabah@gmail.com abdeldjalil.aissaelbey@imt-atlantique.fr thierry.chonavel@imt-atlantique.fr djeddou.mustapha@gmail.com

Abstract—Orthogonal time frequency space modulation (OTFS) has been proved to have better performance over orthogonal frequency division multiplexing (OFDM) under high-mobility environments. In this manuscript, we address the challenging problem of channel estimation in high-mobility scenarios for 5G and beyond. To improve the spectral efficiency of the system, we combine superimposed pilots with index modulation paradigm. Indeed, we propose an iterative algorithm for channel estimation and symbol detection with superimposed pilot pattern for OTFS-IM systems. The proposed algorithm iterates between LMMSE-based data detection and data-aided channel estimation. Performance in terms of spectral efficiency and bit error rate are evaluated and compared against state-of-the-art methods.

Index Terms—OTFS, index modulation, channel estimation, high-mobility, time-varying channels

I. INTRODUCTION

Reliable communications in high-mobility environments is a challenging problem in future mobile communication systems. OFDM, which is the modulation used in today's mobile-communication systems due to its robustness in time-invariant frequency selective channels, sees its performance deteriorate in high mobility scenarios, such as high-speed trains scenarios, because of severe inter-carrier interference [1].

OTFS modulation has been recently proposed in [2], [3] to deal with time-varying channels. The secret of OTFS is that it transforms a doubly-selective wireless channel to an almost flat one in the delay-Doppler (DD) domain thanks to the inverse symplectic finite Fourier transform (ISFFT). This fact can be exploited to reduce the bit error rate (BER), leading to better performance gain compared to OFDM.

To further increase spectral efficiency (SE), the index modulation (IM) paradigm for OFDM (OFDM-IM) has been extended to OTFS modulation. Several OFDM-IM schemes have been proposed in [4]–[10]. But its performance degrades in high-mobility scenarios. To address this problem, a novel OTFS scheme with IM has been proposed in [11], [12]. Compared to OFDM-IM and OTFS, OTFS-IM has improved BER performance for scenarios involving high mobility and high SE. However, perfect channel state information (CSI) is assumed known in these works. In practice, channel estimation requires the use of pilots, which decreases SE. In addition, considering an imperfect channel estimate decreases the performance of the system.

Several channel estimation schemes in the DD domain for OTFS have been proposed. They can be classified into three groups. The first group, named conventional pilot aided (CPA), uses schemes that employ a super architecture frame, i.e., the first OTFS frame is used for channel estimation and subsequent frames for data transmission [13]–[18]. The second group, called embedded pilot (EP), involves the transmission of both pilots and data symbols in the same frame with guard intervals to avoid interference during channel estimation [19]–[27]. The last group adopts a superimposed scheme, where pilots and data symbols are spread in the DD domain [28]–[30].

In this paper, we propose an iterative algorithm for channel estimation and symbol detection in the DD domain for OTFS-IM systems. To avoid pilot overhead and further improve the SE of the system, we adopt the superimposed pilot pattern. The proposed algorithm, which benefits from the DD channel sparsity, iterates between an LMMSE-based data detection and data-aided channel estimation. Performance of the proposed algorithm in terms of SE and BER are compared against state-of-the-art methods.

II. SYSTEM MODEL

The block diagram of OTFS-IM is shown in Fig 1. We consider an OTFS frame with N symbols and M subcarriers. T , Δf denote the symbol duration and the subcarrier spacing, respectively.

OTFS-IM differs from OFDM-IM systems by carrying index information through a combination of silence and active points on the 2D-DD grid, instead of silent subcarriers. In OTFS-IM, no subcarrier is silent when transformed to the time-frequency domain.

First, the N_b transmitted bits are divided into G groups, each one with $b = N_b/G$ bits. Each group of b bits is then divided into two subgroups, one with b_1 bits referred as index selector and the other with $b_2 = K \log_2(M_a)$ bits mapped into an M_a -ary signal constellation on active index subsets, where K is the number of active indices chosen by the b_1 bits. b_1 is calculated as $b_1 = \text{floor}(\log_2(C_L^K))$, C_L^K being the binomial coefficient. Then, the g -th OTFS subblock of size $L = NM/G$ is formed by means of the Gray-coded pairwise index mapping exemplified in Table I and expressed as:

$$\mathbf{x}_d^{(g)} = [x_d^{(g)}(1), \dots, x_d^{(g)}(L)]^T, \quad 1 \leq g \leq G, \quad (1)$$

where $x_d^{(g)}(i) \in \{0, M_a\}$. Afterwards, all the OTFS subblocks pass through the OTFS Block Generator & Add Pilots to form the DD transmitted signal $\mathbf{X}_{DD} = \mathbf{X}_p + \mathbf{X}_d \in \mathbb{C}^{M \times N}$. Where \mathbf{X}_d is formed by subblocks in (1) and \mathbf{X}_p is the pilot matrix formed by the arrangement of $X_p[k, l]$ for $k = 0 : N - 1$ and $l = 0 : M - 1$. The elements of \mathbf{X}_p and \mathbf{X}_d are assumed independent and identically distributed with zero-mean and we note $\mathbb{E}\{|X_p[k, l]|^2\} = \sigma_p^2$ and $\mathbb{E}\{|X_d[k, l]|^2\} = \sigma_d^2$. Thus, $\mathbb{E}\{|X_{DD}[k, l]|^2\} = \sigma_d^2 + \sigma_p^2 = \sigma_x^2$.

Then, the DD signal \mathbf{X}_{DD} is transformed into a 2D time-frequency signal \mathbf{X}_{TF} via an ISFFT. \mathbf{X}_{TF} is then transformed to the transmitted time domain signal via the Heisenberg transform along with the pulse-shaping waveform $g_{tx}(t)$ [31]:

$$\mathbf{S} = \mathbf{G}_{tx} \mathbf{F}_M^H (\mathbf{F}_M \mathbf{X}_{DD} \mathbf{F}_N^H) = \mathbf{G}_{tx} \mathbf{X}_{DD} \mathbf{F}_N^H, \quad (2)$$

where $\mathbf{G}_{tx} = \text{diag}\{g_{tx}(0), \dots, g_{tx}((M-1)T/M)\} \in \mathbb{C}^{M \times M}$ and \mathbf{F}_K and \mathbf{F}_K^H denote the $(K \times K)$ DFT and IDFT matrices. $\mathbf{S} \in \mathbb{C}^{M \times N}$ is then converted to a 1D signal $\mathbf{s} \in \mathbb{C}^{MN \times 1}$ via a column vectorization procedure. One cyclic prefix (CP) is added to the signal $\mathbf{s}(t)$ before its transmission to avoid inter-symbol interference between OTFS blocks.

Next, the signal $\mathbf{s}(t)$ is transmitted through the multi-paths time-varying wireless channel $h(\tau, \nu)$, which is sparse in the DD domain, involving only a few parameters. Thus, the baseband channel impulse response can be represented as:

$$h(\tau, \nu) = \sum_{i=1}^P h_i \delta(\tau - \tau_i) \delta(\nu - \nu_i), \quad (3)$$

where P is the number of propagation paths, h_i , τ_i , and ν_i denote the complex gain, delay shift, and Doppler shift of the i -th path, respectively. The i -th delay and Doppler taps (l_i, k_i) are defined as $l_i = \tau_i M \Delta f$ and $k_i = \nu_i N T$.

After removing the CP, the received signal becomes $\mathbf{r} = \mathbf{H} \mathbf{s} + \mathbf{v}$, where $\mathbf{H} = \sum_{i=1}^P h_i \mathbf{\Pi}^{l_i} \mathbf{\Delta}^{k_i}$, with $\mathbf{\Delta} = \text{diag}\{\exp(j2\pi(0)/MN), \dots, \exp(j2\pi(MN-1)/MN)\}$ and $\mathbf{\Pi}$ is the right shift permutation matrix. Then, \mathbf{r} is arranged into a matrix $\mathbf{R} \in \mathbb{C}^{M \times N}$ and the Wigner transform with the waveform $g_{rx}(t)$ and the symplectic finite Fourier transform (SFFT) are successively applied yielding $\mathbf{Y}_{DD} = \mathbf{F}_M^H (\mathbf{F}_M \mathbf{G}_{rx} \mathbf{R}) \mathbf{F}_N \in \mathbb{C}^{M \times N}$ in the DD domain. \mathbf{Y}_{DD} can be written in vector form as $\mathbf{y}_{DD} = (\mathbf{F}_N \otimes \mathbf{G}_{rx}) \mathbf{r}$, where $\mathbf{G}_{rx} = \text{diag}\{g_{rx}(0), g_{rx}(T/M), \dots, g_{rx}((M-1)T/M)\} \in \mathbb{C}^{M \times M}$.

Finally, \mathbf{y}_{DD} is sent to the proposed algorithm to estimate the channel, demodulate the index bits and information bits, which will be discussed in details in Section III.

III. PROPOSED SCHEME

A. Problem formulation

The relationship between the received signal and the transmitted data and pilots can be expressed in a vector form as:

$$\mathbf{y}_{DD} = \mathbf{H}_{\text{eff}} \mathbf{x}_p + \mathbf{H}_{\text{eff}} \mathbf{x}_d + \tilde{\mathbf{v}}, \quad (4)$$

TABLE I: A Look-Up Table: $L = 4, K = 2, b_1 = 2$.

b_1 bits	Indices	Subblocks
[0 0]	[1 2]	$[s_1, s_2, 0, 0]$
[0 1]	[2 3]	$[0, s_1, s_2, 0]$
[1 0]	[3 4]	$[0, 0, s_1, s_2]$
[1 1]	[1 4]	$[s_1, 0, 0, s_2]$

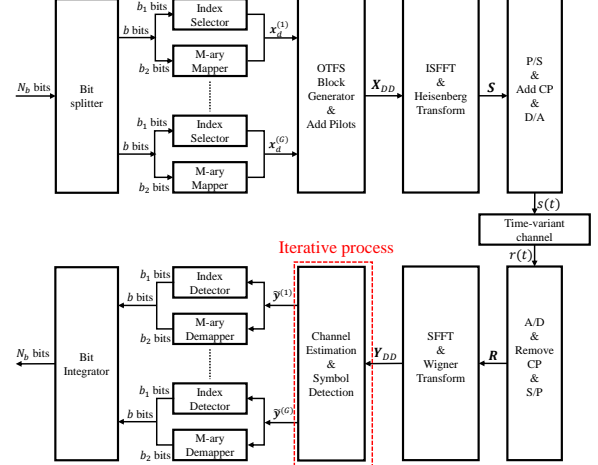


Fig. 1: Block diagram of OTFS-IM system.

where $\mathbf{H}_{\text{eff}} = (\mathbf{F}_N \otimes \mathbf{G}_{rx}) \mathbf{H} (\mathbf{F}_N^H \otimes \mathbf{G}_{tx})$, \mathbf{x}_p and \mathbf{x}_d are the column vectorization of \mathbf{X}_p and \mathbf{X}_d . $\tilde{\mathbf{v}} = (\mathbf{F}_N \otimes \mathbf{G}_{rx}) \mathbf{v}$.

We note $\mathbf{y}_p = \mathbf{H}_{\text{eff}} \mathbf{x}_p = \Phi_p \mathbf{h}$ and $\mathbf{y}_d = \mathbf{H}_{\text{eff}} \mathbf{x}_d = \Phi_d \mathbf{h}$, where $\Phi_p = [\Psi_1 \mathbf{x}_p, \Psi_2 \mathbf{x}_p, \dots, \Psi_P \mathbf{x}_p] \in \mathbb{C}^{MN \times P}$ and $\Phi_d = [\Psi_1 \mathbf{x}_d, \Psi_2 \mathbf{x}_d, \dots, \Psi_P \mathbf{x}_d]$, with $\Psi_i = (\mathbf{F}_N \otimes \mathbf{G}_{rx}) (\mathbf{\Pi}^{l_i} \mathbf{\Delta}^{k_i}) (\mathbf{F}_N^H \otimes \mathbf{G}_{tx}) \in \mathbb{C}^{MN \times MN}$. $\mathbf{h} = [h_1, h_2, \dots, h_P]^T \in \mathbb{C}^{P \times 1}$ has zero mean and covariance matrix $\mathbf{C}_h = \mathbb{E}\{\mathbf{h} \mathbf{h}^H\} = \text{diag}\{\sigma_{h_1}^2, \sigma_{h_2}^2, \dots, \sigma_{h_P}^2\}$.

Finally, channel estimation in this context amounts to finding the channel support $\{l_i, k_i\}$ as well as the corresponding path parameters $\{h_i, \tau_i, \nu_i\}$ for $i = 1 : P$. Whereas, symbol detection amounts to finding data vector \mathbf{x}_d from (4). Since $\{l_i, k_i\}$ remain unchanged for a period T_s , for a doubly-underspread (DU) channel [32], the estimation of these parameters is done once every $T_s = N_T T$ seconds, where N_T is the number of frames in the period T_s .

B. OTFS-IM-SNI algorithm

Here, we present the proposed superimposed pilot non-iterative (SNI) algorithm for channel estimation and symbol detection in OTFS-IM (OTFS-IM-SNI). By considering data as interference, the received signal in (4) can be rewritten as:

$$\mathbf{y}_{DD} = \Phi_p \mathbf{h} + \tilde{\mathbf{v}}_d, \quad (5)$$

where $\tilde{\mathbf{v}}_d = \mathbf{H}_{\text{eff}} \mathbf{x}_d + \tilde{\mathbf{v}}$. The mean and the covariance matrix of $\tilde{\mathbf{v}}_d$ are expressed as $\mu_{\tilde{\mathbf{v}}_d} = \mathbb{E}\{\tilde{\mathbf{v}}_d\} = \mathbf{0}_{MN \times 1}$ and $\mathbf{C}_{\tilde{\mathbf{v}}_d} = \mathbb{E}\{\tilde{\mathbf{v}}_d \tilde{\mathbf{v}}_d^H\} = \left(\left(\sum_{i=1}^P \sigma_{h_i}^2 \right) \sigma_d^2 + \sigma_v^2 \right)$ [29], [30].

Using the observation model (5), the estimate $\hat{\mathbf{h}}_{\text{SNI}}$ of \mathbf{h} is derived via an MMSE estimator as follows:

$$\hat{\mathbf{h}}_{\text{SNI}} = (\Phi_p^H \mathbf{C}_{\tilde{\mathbf{v}}_d}^{-1} \Phi_p + \mathbf{C}_h^{-1})^{-1} \Phi_p^H \mathbf{C}_{\tilde{\mathbf{v}}_d}^{-1} \mathbf{y}_{DD}. \quad (6)$$

Note that this estimator exploits the DD sparsity by computing the inverse of a $P \times P$ matrix, where $P \ll MN$.

Next, we use an MMSE algorithm to detect the symbol vector \mathbf{x}_d . The signal used for symbol detection is obtained by subtracting the estimated pilot signal from (4) as follows:

$$\mathbf{y}_d = \mathbf{y}_{DD} - \hat{\mathbf{H}}_{\text{eff-SNI}} \mathbf{x}_p = \mathbf{H}_{\text{eff}} \mathbf{x}_d + \tilde{\mathbf{v}}_e, \quad (7)$$

where $\tilde{\mathbf{v}}_e = (\mathbf{H}_{\text{eff}} - \hat{\mathbf{H}}_{\text{eff-SNI}}) \mathbf{x}_p + \tilde{\mathbf{v}}$. Since $(\mathbf{H}_{\text{eff}} - \hat{\mathbf{H}}_{\text{eff-SNI}}) \mathbf{x}_p$ and $\tilde{\mathbf{v}}$ are statistically independent, the mean and variance of the entries of $\tilde{\mathbf{v}}_e$ are given as $\mu_{\tilde{\mathbf{v}}_e(i)} = \mathbb{E}\{\tilde{\mathbf{v}}_e(i)\} = 0$ and $\text{var}\{\tilde{\mathbf{v}}_e(i)\} = \sigma_v^2 + \sigma_p^2 \mathbb{E}\{\|\mathbf{h} - \hat{\mathbf{h}}_{\text{SNI}}\|^2\}$ [29].

From (7), the MMSE estimate of \mathbf{x}_d is given as follows:

$$\hat{\mathbf{x}}_d = (\hat{\mathbf{H}}_{\text{eff-SNI}}^H \hat{\mathbf{H}}_{\text{eff-SNI}} + \lambda \mathbf{I}_{MN})^{-1} \hat{\mathbf{H}}_{\text{eff-SNI}}^H \mathbf{y}_d, \quad (8)$$

where $\lambda = \sigma_v^2 + \sigma_p^2 \mathbb{E}\{\|\mathbf{h} - \hat{\mathbf{h}}_{\text{SNI}}\|^2\}$. As $\mathbf{A} = (\hat{\mathbf{H}}_{\text{eff-SNI}}^H \hat{\mathbf{H}}_{\text{eff-SNI}} + \lambda \mathbf{I}_{MN})$ is a bounded Hermitian matrix with a lower and upper bound P , we propose a low complexity MMSE (LMMSE) by computing \mathbf{A}^{-1} via \mathbf{LDL}^H decomposition. Therefore, $\hat{\mathbf{x}}_d$ is obtained as follows: compute $\mathbf{A} = \mathbf{LDL}^H \rightarrow$ solve $\mathbf{L}\mathbf{s}_1 = \hat{\mathbf{H}}_{\text{eff-SNI}}^H \mathbf{y}_d \rightarrow$ solve $\mathbf{D}\mathbf{s}_2 = \mathbf{s}_1 \rightarrow$ solve $\mathbf{L}^H \mathbf{s}_3 = \mathbf{s}_2 \rightarrow$ obtain $\hat{\mathbf{x}}_d = \mathbf{s}_3$.

The estimator in (8) allows to detect both constellation symbols and indices bits. To obtain the sequence of bits sent, we first use a power detection technique for only detecting the power of indices information. This technique consists in detecting the indices of the k most powerful entries of vectors $\tilde{\mathbf{y}}^{(g)} = [\hat{\mathbf{x}}_d^{(g)}((g-1)L+1), \dots, \hat{\mathbf{x}}_d^{(g)}((g-1)L+L)]$ for $g = 1 : G$. These estimated indices allow us to reconstitute the sequence of bits sent using Table 1.

C. OTFS-IM-SI algorithm

The performance of OTFS-IM-SNI degrades for high SNR, as shown in Section. IV. To address this problem, we propose a superimposed pilot iterative (SI) algorithm which iterates between channel estimation and symbol detection, named OTFS-IM-SI. It begins with the symbol estimate $\hat{\mathbf{x}}_d^{(0)} = \hat{\mathbf{x}}_{d\text{-SNI}}$ obtained from OTFS-IM-SNI. With $\hat{\mathbf{x}}_d^{(0)}$, we can compute an initial estimate of Φ_d as $\hat{\Phi}_d^{(0)} = [\Psi_1 \hat{\mathbf{x}}_d^{(0)}, \Psi_2 \hat{\mathbf{x}}_d^{(0)}, \dots, \Psi_P \hat{\mathbf{x}}_d^{(0)}]$. The received signal expression (4) can be rewritten as follows:

$$\mathbf{y}_{DD} = \hat{\Phi}_{\hat{\mathbf{x}}_d, \mathbf{x}_p}^{(0)} \mathbf{h} + \gamma_{\tilde{\mathbf{v}}}^{(0)}, \quad (9)$$

where $\hat{\Phi}_{\hat{\mathbf{x}}_d, \mathbf{x}_p}^{(0)} = \Phi_p + \hat{\Phi}_d^{(0)}$ is the data-aided matrix and $\gamma_{\tilde{\mathbf{v}}}^{(0)} = (\Phi_d - \hat{\Phi}_d^{(0)}) \mathbf{h} + \tilde{\mathbf{v}}$ denote the noise-plus-interference vector. $\gamma_{\tilde{\mathbf{v}}}^{(0)}$ has a zero mean and a covariance matrix $\mathbf{C}_{\gamma_{\tilde{\mathbf{v}}}^{(0)}} = 2 \left(\sum_{i=1}^P \sigma_{h_i^2} \right) \sigma_d^2 + \sigma_v^2 \mathbf{I}_{MN}$ [29].

The estimate of \mathbf{h} in the n -th iteration of the OTFS-IM-SI is expressed as follows:

$$\hat{\mathbf{h}}_{\text{SI}}^{(n)} = \Gamma^{(n)} \left(\hat{\Phi}_{\hat{\mathbf{x}}_d, \mathbf{x}_p}^{(n-1)} \right)^H \left(\mathbf{C}_{\gamma_{\tilde{\mathbf{v}}}^{(n-1)}} \right)^{-1} \mathbf{y}_{DD}, \quad (10)$$

where $\Gamma^{(n)} = \left(\left(\hat{\Phi}_{\hat{\mathbf{x}}_d, \mathbf{x}_p}^{(n-1)} \right)^H \left(\mathbf{C}_{\gamma_{\tilde{\mathbf{v}}}^{(n-1)}} \right)^{-1} \hat{\Phi}_{\hat{\mathbf{x}}_d, \mathbf{x}_p}^{(n-1)} + \mathbf{C}_h^{-1} \right)^{-1}$.

Once \mathbf{h} is estimated, we can compute the effective channel matrix in the n -th iteration as $\hat{\mathbf{H}}_{\text{eff-SI}}^{(n)} = (\mathbf{F}_N \otimes \mathbf{G}_{rx}) \left(\sum_{i=1}^P \hat{h}_i^{(n)} \mathbf{\Pi}^i \mathbf{\Delta}^{k_i} \right) (\mathbf{F}_N^H \otimes \mathbf{G}_{tx})$.

We now use the proposed LMMSE estimator in (8) to detect symbols vector. The received signal for symbol detection at the n -th iteration of the OTFS-IM-SI is obtained as follows:

$$\mathbf{y}_d^{(n)} = \mathbf{y}_{DD} - \hat{\mathbf{H}}_{\text{eff-SI}}^{(n)} \mathbf{x}_p = \mathbf{H}_{\text{eff}} \mathbf{x}_d + \tilde{\mathbf{v}}_e^{(n)}, \quad (11)$$

where $\tilde{\mathbf{v}}_e^{(n)} = (\mathbf{H}_{\text{eff}} - \hat{\mathbf{H}}_{\text{eff-SI}}^{(n)}) \mathbf{x}_p + \tilde{\mathbf{v}}$. Note that $\mu_{\tilde{\mathbf{v}}_e^{(n)}(i)} = \mathbb{E}\{\tilde{\mathbf{v}}_e^{(n)}(i)\} = 0$ and $\text{var}\{\tilde{\mathbf{v}}_e^{(n)}(i)\} = \sigma_v^2 + \sigma_p^2 \mathbb{E}\{\|\mathbf{h} - \hat{\mathbf{h}}_{\text{SI}}^{(n)}\|^2\}$.

From (11), the LMMSE estimate of the symbol vector \mathbf{x}_d is given as follows:

$$\hat{\mathbf{x}}_d^{(n)} = \left(\left(\hat{\mathbf{H}}_{\text{eff-SI}}^{(n)} \right)^H \hat{\mathbf{H}}_{\text{eff-SI}}^{(n)} + \lambda^{(n)} \mathbf{I}_{MN} \right)^{-1} \left(\hat{\mathbf{H}}_{\text{eff-SI}}^{(n)} \right)^H \mathbf{y}_d^{(n)}, \quad (12)$$

where $\lambda^{(n)} = \sigma_v^2 + \sigma_p^2 \mathbb{E}\{\|\mathbf{h} - \hat{\mathbf{h}}_{\text{SI}}^{(n)}\|^2\}$. As for OTFS-IM-SNI, the inverse of $\mathbf{A}^{(n)} = \left(\left(\hat{\mathbf{H}}_{\text{eff-SI}}^{(n)} \right)^H \hat{\mathbf{H}}_{\text{eff-SI}}^{(n)} + \lambda^{(n)} \mathbf{I}_{MN} \right)$ is calculated using \mathbf{LDL}^H decomposition.

OTFS-IM-SI iterates between data-aided channel estimation in (10) and MMSE-based data detection in (12) and stops when $|\hat{\mathbf{h}}^{(n)} - \hat{\mathbf{h}}^{(n-1)}| < \epsilon$ or when the maximum number of iterations N_{max} is reached.

From the detected vector $\hat{\mathbf{x}}_d$, we form the OTFS sub-blocks. Then, we use the power detection technique for detecting the power of indices information, which allows to reconstitute the sequence of bits sent using Table I.

IV. SIMULATION RESULTS

Here, we present the performance of the proposed algorithm in terms of SE and BER under high-mobility conditions. Then we compare these performance against state-of-the-art methods: CPA design [18], EP scheme [19], No guard in the right side (NGR) method [26], Bayesian learning based row and group sparse (RG-BL) method [33], block sparse Bayesian learning with block reorganization (BSBL-BR) method [24], OFDM-IM-perfect-CSI, and OTFS-IM-perfect-CSI.

A. Simulation parameters

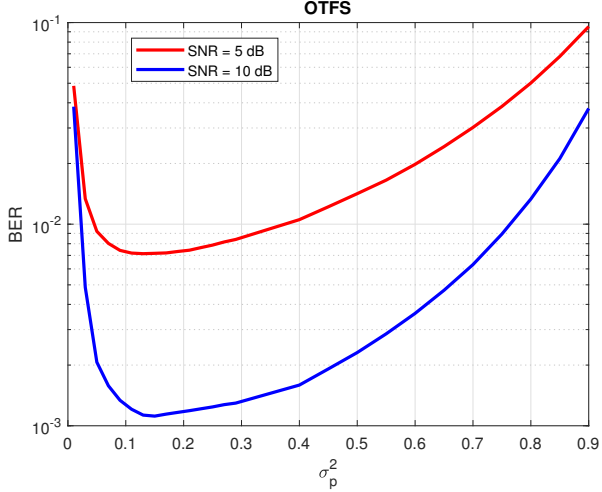
Simulation parameters are given in Table II. Similar to [18], we use the 5-path DD channel model whose parameters are given in [29]. The maximum delay shift is $\tau_{max} = 20.8 \mu\text{s}$, which corresponds to a maximum delay tap $l_\tau = 5$. The maximum Doppler shift is $\nu_{max} = 1850 \text{ Hz}$, which corresponds to a high-mobility scenario with maximum Doppler tap $k_\nu = 2$ and a maximum speed of $v_{max} = 500 \text{ km/h}$.

For a fair comparison with the state-of-the-art schemes, the total power per frame must remain the same for each scheme. Here, this power is fixed to MN .

We can check that the used channel is a doubly under-spread channel [29]. The number of frames N_f in which the delay and Doppler taps remain constant is $N_f = T_s/T_f$, where $T_f =$

TABLE II: Simulation parameters.

Parameter	Value	Parameter	Value
M, N	16, 16	G, L, K, b_1	64, 4, 4, 2
$f_c(\text{GHz}), \Delta f(\text{kHz})$	4, 15	P	5
Modulation	QPSK	Pulse shaping	rectangular


 Fig. 2: BER versus σ_p^2 performance for OTFS-IM-SI.

$N/\Delta f$ is the frame duration. Here, $N_f \approx 10$. N_f increases as v_{max} decreases, e.g. for $v_{max} = 250$ km/h, $N_f \approx 20$.

Here, we first estimate $\{l_i, k_i\}_{i=1:P}$ using the simple threshold method and the NGR scheme in [26] in the first frame, then in the $N_f - 1$ other frames we use the proposed algorithm for only estimate $\{h_i\}_{i=1:P}$. Therefore, the SE expression can be computed as $R_{\text{OTFS-IM-SI}} = (\mathcal{R}_{\text{NGR}} + (N_f - 1)\mathcal{R}_{\text{OTFS-IM}})/N_f$, where \mathcal{R}_{NGR} and $\mathcal{R}_{\text{OTFS-IM}}$ are the SE of the NGR and OTFS-IM schemes whose expressions are given in Table III.

B. Pilots/Data optimal power allocation

The allocated pilots power influences the performance of the system. This led us to investigate the variation of BER versus σ_p^2 by varying σ_p^2 in the interval $[0.01; 0.9]$, as shown in Fig 2. We observe that the minimum BER is achieved at approximately $\sigma_p^2 = \sigma_{opt}^2 = 15\%$. The BER degradation away from σ_{opt}^2 is due to a poor channel estimation if $\sigma_p^2 < \sigma_{opt}^2$ and is due to the reduced data power ($\sigma_d^2 = 1 - \sigma_p^2$) if $\sigma_p^2 > \sigma_{opt}^2$.

C. SE analysis

We now compare the SE of OTFS-IM-SI against state-of-the-art methods, as shown in Table III. As there is no pilot overhead in the proposed scheme, due to the superposition of pilots and data symbols, the SE reaches those of OTFS-IM and OFDM-IM systems with perfect CSI. For the OFDM-IM with channel estimation, the SE degrades due to pilot overhead. From Table III, we observe that the proposed scheme performs better in terms of SE compared to all state-of-the-art methods. This is due to the fact that the SE of OTFS-IM contains both indices part and constellation symbols part.

 TABLE III: SE comparison between OTFS-IM-SI and state-of-the-art methods ($M = N = 16$, $N_p = 4$, $M_a = 4$, $L = 4$, $K = 3$, $L_p = 30$, and $N_G = 98$, $v_{max} = 250, 500$ km/h).

Design	SE expression	SE value
CPA [18]	$(MN/2MN) \log_2(M_a)$	1 bits/s/Hz
EP [19]	$(MN - N_G - 1)/MN \log_2(M_a)$	1.23 bits/s/Hz
RG-BL [33]	$(N/(N_p + N)) \log_2(M_a)$	1.60 bits/s/Hz
BSBL-BR [24] NGR [26]	$((MN - L_p)/MN) \log_2(M_a)$	1.77 bits/s/Hz
OTFS-IM	$\frac{1}{L} \log_2(C_L^K) + \frac{K}{L} \log_2(M_a)$	2 bits/s/Hz
SI (500 km/h) SI (250 km/h)	$\frac{\mathcal{R}_{\text{NGR}} + (N_f - 1)\mathcal{R}_{\text{OTFS-IM}}}{N_f}$	1.98 bits/s/Hz 1.99 bits/s/Hz

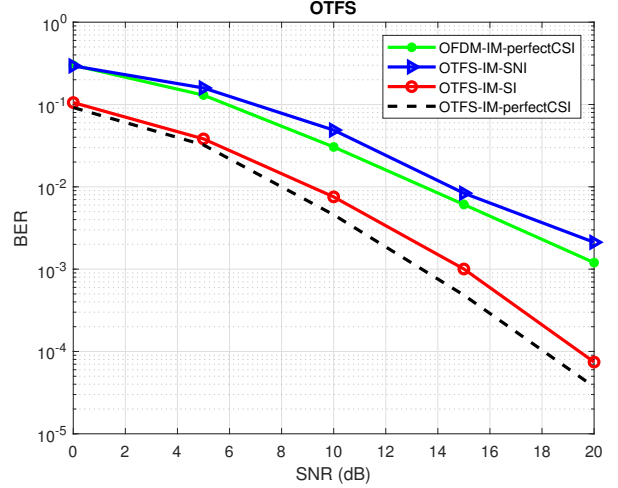


Fig. 3: BER versus SNR performance.

D. BER analysis

We now investigate the variation of BER versus SNR. Fig 3 shows the BER over SNR performance of the proposed schemes and OFDM-IM and OTFS-IM with perfect CSI. From Fig 3, we observe that OTFS-IM-SNI and OFDM-IM with perfect CSI perform almost similarly at low SNR values. At high SNR, the BER performance of OTFS-IM-SNI saturates. This is due to the interference introduced by the pilots. We also observe that OTFS-IM-SI outperforms all the other methods and has a close performance to the oracle. It exceeds the OFDM-IM with perfect CSI by about 5 dB at $\text{BER} = 10^{-4}$.

V. CONCLUSION

In this paper, we have addressed the channel estimation problem in high mobility scenarios for OTFS systems. To increase the spectral efficiency of the system, two paradigms have been brought into play: index modulation and the superposition of pilots and data symbols. We have proposed an iterative channel estimation and data detection algorithm. The proposed algorithm iterates between LMMSE-based data detection and data-aided channel estimation. Simulation results show that the proposed scheme outperforms the state-of-the-art methods in terms of spectral efficiency and bit error rate under high mobility environments.

REFERENCES

- [1] P. Singh, A. Gupta, H. B. Mishra, and R. Budhiraja, "Low-complexity ZF/MMSE MIMO-OTFS receivers for high-speed vehicular communication," *IEEE Open Journal of the Communications Society*, vol. 3, pp. 209–227, 2022.
- [2] A. Monk, R. Hadani, M. Tsatsanis, and S. Rakib, "OTFS-orthogonal time frequency space," *arXiv preprint arXiv:1608.02993*, 2016.
- [3] R. Hadani, S. Rakib, M. Tsatsanis, A. Monk, A. J. Goldsmith, A. F. Molisch, and R. Calderbank, "Orthogonal time frequency space modulation," in *2017 IEEE Wireless Communications and Networking Conference (WCNC)*, pp. 1–6.
- [4] R. Abu-Alhiga and H. Haas, "Subcarrier-index modulation OFDM," in *2009 IEEE 20th International Symposium on Personal, Indoor and Mobile Radio Communications*, pp. 177–181.
- [5] D. Tsonev, S. Sinanovic, and H. Haas, "Enhanced subcarrier index modulation (SIM) OFDM," in *2011 IEEE GLOBECOM Workshops (GC Wkshps)*, pp. 728–732.
- [6] E. Başar, Ü. Aygözü, E. Panayırıcı, and H. V. Poor, "Orthogonal frequency division multiplexing with index modulation," *IEEE Transactions on signal processing*, vol. 61, no. 22, pp. 5536–5549, 2013.
- [7] T. Mao, Z. Wang, Q. Wang, S. Chen, and L. Hanzo, "Dual-mode index modulation aided OFDM," *IEEE Access*, vol. 5, pp. 50–60, 2016.
- [8] X. Zhang, H. Bie, Q. Ye, C. Lei, and X. Tang, "Dual-mode index modulation aided OFDM with constellation power allocation and low-complexity detector design," *IEEE access*, vol. 5, pp. 23 871–23 880, 2017.
- [9] M. I. Kadir, "Generalized space–time–frequency index modulation," *IEEE Communications Letters*, vol. 23, no. 2, pp. 250–253, 2018.
- [10] S. Sugiura, T. Ishihara, and M. Nakao, "State-of-the-art design of index modulation in the space, time, and frequency domains: Benefits and fundamental limitations," *IEEE Access*, vol. 5, pp. 21 774–21 790, 2017.
- [11] Y. Liang, L. Li, P. Fan, and Y. Guan, "Doppler resilient orthogonal time-frequency space (OTFS) systems based on index modulation," in *2020 IEEE 91st Vehicular Technology Conference (VTC2020-Spring)*, pp. 1–5.
- [12] H. Zhao, D. He, Z. Kang, and H. Wang, "Orthogonal time frequency space (OTFS) with dual-mode index modulation," *IEEE Wireless Communications Letters*, vol. 10, no. 5, pp. 991–995, 2021.
- [13] I. A. Khan and S. K. Mohammed, "Low complexity channel estimation for OTFS modulation with fractional delay and doppler," *arXiv preprint arXiv:2111.06009*, 2021.
- [14] M. Zhang, F. Wang, X. Yuan, and L. Chen, "2D structured turbo compressed sensing for channel estimation in OTFS systems," in *2018 IEEE International Conference on Communication Systems (ICCS)*, pp. 45–49.
- [15] O. K. Rasheed, G. Surabhi, and A. Chockalingam, "Sparse delay-doppler channel estimation in rapidly time-varying channels for multiuser OTFS on the uplink," in *2020 IEEE 91st Vehicular Technology Conference (VTC2020-Spring)*, pp. 1–5.
- [16] F. Gómez-Cuba, "Compressed sensing channel estimation for OTFS modulation in non-integer delay-doppler domain," in *2021 IEEE Global Communications Conference (GLOBECOM)*, pp. 1–6.
- [17] K. Murali and A. Chockalingam, "On OTFS modulation for high-doppler fading channels," in *2018 Information Theory and Applications Workshop (ITA)*, pp. 1–10.
- [18] M. K. Ramachandran and A. Chockalingam, "MIMO-OTFS in high-doppler fading channels: Signal detection and channel estimation," in *2018 IEEE Global Communications Conference (GLOBECOM)*, pp. 206–212.
- [19] P. Raviteja, K. T. Phan, and Y. Hong, "Embedded pilot-aided channel estimation for OTFS in delay–doppler channels," *IEEE Transactions on vehicular technology*, vol. 68, no. 5, pp. 4906–4917, 2019.
- [20] W. Shen, L. Dai, J. An, P. Fan, and R. W. Heath, "Channel estimation for orthogonal time frequency space (OTFS) massive MIMO," *IEEE Transactions on Signal Processing*, vol. 67, no. 16, pp. 4204–4217, 2019.
- [21] Y. Liu, S. Zhang, F. Gao, J. Ma, and X. Wang, "Uplink-aided high mobility downlink channel estimation over massive MIMO-OTFS system," *IEEE Journal on Selected Areas in Communications*, vol. 38, no. 9, pp. 1994–2009, 2020.
- [22] L. Zhao, W.-J. Gao, and W. Guo, "Sparse Bayesian learning of delay-Doppler channel for OTFS system," *IEEE Communications letters*, vol. 24, no. 12, pp. 2766–2769, 2020.
- [23] H. Qu, G. Liu, L. Zhang, M. A. Imran, and S. Wen, "Low-dimensional subspace estimation of continuous-doppler-spread channel in OTFS systems," *IEEE Transactions on communications*, vol. 69, no. 7, pp. 4717–4731, 2021.
- [24] L. Zhao, J. Yang, Y. Liu, and W. Guo, "Block sparse bayesian learning-based channel estimation for MIMO-OTFS systems," *IEEE Communications Letters*, vol. 26, no. 4, pp. 892–896, 2022.
- [25] G. Guo, Z. Jin, X. Zhang, and J. Wei, "Joint iterative channel estimation and symbol detection for orthogonal time frequency space modulation," in *2021 IEEE 94th Vehicular Technology Conference (VTC2021-Fall)*, pp. 1–6.
- [26] R. Liu, Y. Huang, D. He, Y. Xu, and W. Zhang, "Optimizing channel estimation overhead for OTFS with prior channel statistics," in *2021 IEEE Wireless Communications and Networking Conference (WCNC)*, pp. 1–6.
- [27] R. Ouchikh, A. Aïssa-El-Bey, T. Chonavel, and M. Djeddou, "Sparse channel estimation algorithms for OTFS system," *IET Communications*, vol. 16, no. 18, pp. 2158–2170, 2022.
- [28] W. Yuan, S. Li, Z. Wei, J. Yuan, and D. W. K. Ng, "Data-aided channel estimation for OTFS systems with superimposed pilot and data transmission scheme," *IEEE Wireless communications letters*, vol. 10, no. 9, pp. 1954–1958, 2021.
- [29] H. B. Mishra, P. Singh, A. K. Prasad, and R. Budhiraja, "OTFS channel estimation and data detection designs with superimposed pilots," *IEEE Transactions on wireless communications*, vol. 21, no. 4, pp. 2258–2274, 2021.
- [30] R. Ouchikh, A. Aïssa-El-Bey, T. Chonavel, and M. Djeddou, "Iterative channel estimation and data detection algorithm for OTFS modulation," in *2022 IEEE International Conference on Acoustics, Speech and Signal Processing (ICASSP)*, pp. 5263–5267.
- [31] P. Raviteja, Y. Hong, E. Viterbo, and E. Biglieri, "Practical pulse-shaping waveforms for reduced-cyclic-prefix OTFS," *IEEE Transactions on Vehicular Technology*, vol. 68, no. 1, pp. 957–961, 2018.
- [32] G. Matz, "On non-WSSUS wireless fading channels," *IEEE Transactions on wireless communications*, vol. 4, no. 5, pp. 2465–2478, 2005.
- [33] S. Srivastava, R. K. Singh, A. K. Jagannatham, and L. Hanzo, "Bayesian learning aided simultaneous row and group sparse channel estimation in orthogonal time frequency space modulated MIMO systems," *IEEE Transactions on Communications*, vol. 70, no. 1, pp. 635–648, 2021.